

In-Hand Manipulation of Articulated Tools with Dexterous Robot Hands with Sim-to-Real Transfer

Soofiyan Atar¹, Daniel Huang¹, Florian Richter¹, Michael Yip¹, *Senior Member, IEEE*

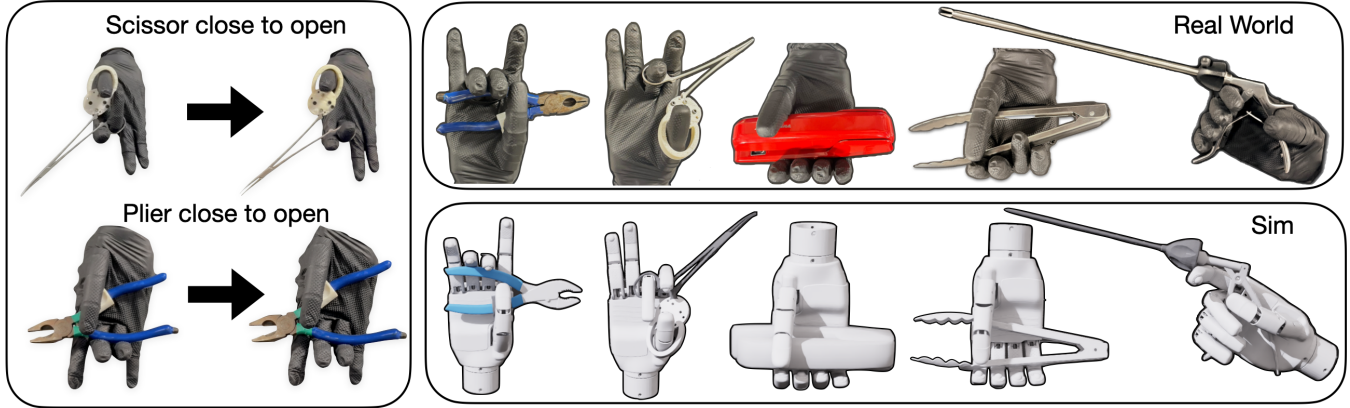


Fig. 1: Left—open-close mechanics of scissors and pliers. Right—real-world and simulation grasp poses, showing alignment of digital clones with physical interactions.

Abstract—Reinforcement learning (RL) and sim-to-real transfer have advanced robotic manipulation of rigid objects. Yet, policies remain brittle when applied to articulated mechanisms due to contact-rich dynamics and under-modeled joint phenomena such as friction, stiction, backlash, and clearances. We address this challenge through dexterous in-hand manipulation of articulated tools using a robotic hand with reduced articulation and kinematic redundancy relative to the human hand. Our controller augments a simulation-trained base policy with a sensor-driven refinement learned from hardware demonstrations, conditioning on proprioception and target articulation states while fusing whole-hand tactile and force feedback with the policy’s internal action intent via cross-attention-based integration. This design enables online adaptation to instance-specific articulation properties, stabilizes contact interactions, regulates internal forces, and coordinates coupled-link motion under perturbations. We validate our approach across a diversity of real-world examples, including scissors, pliers, minimally invasive surgical tools, and staplers. We achieve robust transfer from simulation to hardware, improved disturbance resilience, and generalization to previously unseen articulated tools, thereby reducing reliance on precise physical modeling in contact-rich settings. Website.

I. INTRODUCTION

A primary goal in robotics is to develop robots that can operate effectively in human-centric environments [1]. A key aspect of this is the ability to interact with tools designed for human hands, allowing robots to move beyond factory automation and deliver versatile performance in everyday settings. Although substantial progress has been made in manipulating rigid objects [2], [3], [4], [5], handling articulated tools (i.e., objects with internal kinematics, such as

scissors or pliers) remains especially hard. Humanoid robots are particularly motivated to solve this challenge [6], [7], [8], since they aim to use tools, perform household chores, and work in environments built for people [9], [10]. Advancing in-hand manipulation of articulated tools is thus a critical step toward greater robotic dexterity, broadened real-world capability, and fulfilling the promise of humanoids in human environments [11].

The prevailing paradigm for training dexterous hands is sim-to-real policy transfer [3], [12], [13], where skills are learned in simulation and then deployed on hardware, leveraging simulation as a low-cost data source [14]. This approach has proven effective for tasks involving rigid objects and suction grippers [2], [3], [15], [16], [17]. However, residual reality gaps become pronounced when applied to dynamic, contact-rich tasks—particularly those involving articulated tools. Internal joint interactions, friction, stiction, and other contact phenomena are challenging to model faithfully, undermining the reliability and consistency of transferred policies. Articulated tools add further complexity through joint-dependent dynamics and contact constraints, widening the sim-to-real gap and diminishing policy effectiveness. In such settings, tactile feedback is often essential to perceive object state, such as shear forces or joint motion [18], [19], [20], with visuo-tactile integration offering additional benefits [21]. However, even with these observations, there remains a significant gap in the simulators to accurately represent multi-body dynamical contact under complex nonlinear constraints while meeting kinematic and dynamical constraints, all resulting in poor convergence or brittle simulation [22], [23].

Beyond sim-to-real transfer, other learning-based strate-

¹Electrical and Computer Engineering Department, University of California, San Diego, La Jolla, CA 92093 USA. {satar, yah032, frichter, yip}@ucsd.edu

gies have been explored for dexterous manipulation. Imitation learning [24], [25] and foundation models [26] leverage human demonstrations to guide policy training. Demonstration data are often collected via teleoperation with dexterous hands, sometimes enhanced with haptic feedback [27], [28], [29]. While effective, these approaches face limited scalability due to the high cost and time required for demonstration collection. Another direction is hierarchical policy learning and task planning [30], [31], which decomposes complex skills into structured sub-tasks. However, when low-level skills fail to provide accurate or robust feedback, minor execution errors cascade upward, ultimately degrading the performance of higher-level plans.

To address these challenges, we advance learning-based in-hand manipulation by demonstrating that dexterous robotic hands can effectively manipulate articulated tools. A sim-to-real training pipeline with targeted real-world adaptation is proposed to address the challenges of real-world transfer. As in prior work, we first train a privileged (“oracle”) policy in simulation and distill it into a base (student) policy. One strategy we propose is to augment simulation with random walk force-torque perturbations to mimic gravity-induced and external disturbances (forces/torques) that one would expect when using an articulated tool interaction. Despite these measures, the distilled policy requires additional aid in training for handling unmodeled, contact-rich settings. To address this need, we introduce a Cross-Attention Tactile Force Adaptation (CATFA) module, which fuses the policy’s internal intent embedding (from the frozen base policy) with real tactile and force-torque feedback via multi-head cross-attention. The adapter directly outputs action commands and is trained via behavior cloning on several successful hardware rollouts, eliminating the need for large teleoperation datasets. By conditioning on observed contact signatures, our method achieves fast, closed-loop adaptation to real dynamics, enabling reliable manipulation of articulated tools. Our approach is closely related to CROSS-GAI_T [32], which demonstrates improved generalization to unseen environments through cross-attention over multimodal inputs.

We evaluate our approach in simulation and on a physical Franka arm with a dexterous hand. We use randomized force-torque perturbations in simulation to test how disturbances affect oracle policy stability and trajectory quality. We then run random real-world trajectories with tactile and force-torque sensing, labeling successes via human feedback. These rollouts are incorporated into the online training of CATFA. For evaluation, we benchmark against standard sim-to-real transfer and proprioception-based behavior cloning baselines. CATFA demonstrates consistent improvements in grasp stability and robustness, with qualitative performance maintained across variations in object scale, geometry, and category, including articulated tools that match those used during policy training.

II. RELATED WORKS

In-hand manipulation [33], [34], [35], [36], [37], [38], [39], [40] has seen significant progress through reinforce-

ment learning (RL) within a sim-to-real framework [2], [3]. Seminal works [41] in reorienting a rigid cube and demonstrating dynamic pen spinning have shown that complex skills can be learned entirely in simulation. These methods typically rely on extensive domain randomization to train policies that are robust enough for zero-shot or open-loop transfer to the real world [42], [43]. However, this approach often proves brittle, as the policies still struggle to overcome the reality gap caused by unmodeled, contact-rich physics.

Recent work shows that input representations such as point clouds can considerably improve generalization to novel objects using multi-fingered hands, achieving sim-to-real transfer with minimal real-world tuning [44]. Similarly, methods that use vision-based policies for agile in-hand manipulation on anthropomorphic hands can outperform prior vision baselines when trained under diverse simulation perturbations [45]. Also, the benefit of using rich tactile feedback [46] has shown zero-shot transfer of rotational manipulation tasks for unseen objects under varying contact conditions.

Separately, a significant body of research has focused on the broader challenge of articulated object manipulation, with an emphasis on tasks like opening doors, drawers, and cabinets. Prominent works [47], [48], [49] have successfully trained single, general-purpose policies that map visual inputs (typically point clouds) to robot arm actions, enabling zero-shot transfer to a variety of unseen objects. These methods have made great strides in solving the perception and motion planning problems associated with interacting with articulated mechanisms in the environment. However, these approaches treat the articulated object as part of the static world and do not address the distinct and more dynamic challenge of in-hand manipulation, where the object is held and controlled entirely within the grasp of a dexterous hand, thereby requiring the palm and fingers to achieve both objectives of stable grasp but also articulability of the object.

The challenge of in-hand manipulation is amplified for articulated tools, whose internal dynamics are complex to simulate. Simple cases, such as power tools with a single trigger finger, allow grasp and articulation to be decoupled. Still, tools like scissors or laparoscopic instruments involve coupled motions that create complex contact interactions. Recent work on tweezer manipulation [50] has shown progress, but remains limited to a single tool and relies on privileged controllers, reducing generalizability and bypassing the challenge of online skill discovery. In contrast, our approach introduces a post-transfer adaptation mechanism that learns robust, generalizable policies directly from real-world interaction.

Because of the complexities of in-hand manipulation of articulated tools and the limited observations available from in-hand cameras, the importance of tactile feedback [51] quickly becomes important. Yet, far fewer recent works explore non-vision-based tactile skin simulation that captures both normal and shear forces in a realistic manner. Some simulate simplified skin deformation [52], [53] and sensor response handling, cross-talk, and noise, but remain in-

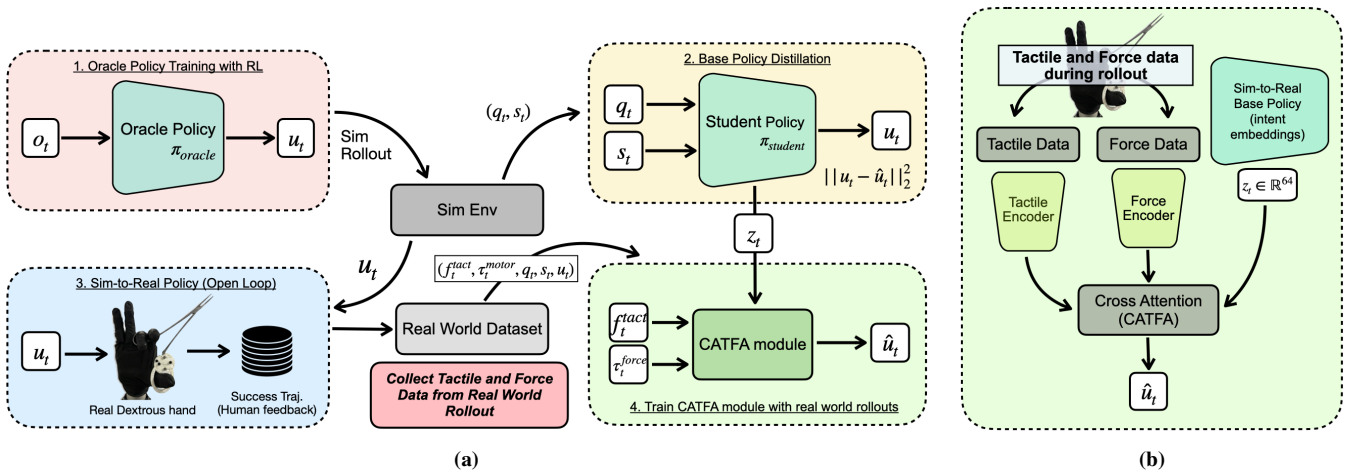


Fig. 2: Pipeline for articulated in-hand manipulation. (a) Oracle training with privileged observations in simulation, followed by distillation into a proprioceptive base policy and data collection with additional tactile f_t^{tact} and motor torque τ_t^{motor} observations. (b) CATFA fuses these modalities with policy intent via cross-attention for online adaptation on hardware.

tractable for training reinforcement learning policies. Others use binary or coarse tactile sensors (e.g., force-sensitive resistors), and other simulators do not represent shear dynamics under contact [54], [19]. In contrast, our work employs whole-hand tactile sensing, providing quantized continuous force readings, which are structured into a tactile image and embedded before cross-attention conditioning of the BC policy.

III. METHODS

We study in-hand manipulation of articulated tools, where a dexterous multi-fingered robotic hand must control an articulated tool with an internal revolute joint $\theta_t^{art} \in \mathbb{R}$ and angular velocity $\dot{\theta}_t^{art} \in \mathbb{R}$, representing the tool’s open/close motion. This setting poses unique challenges due to coupled kinematic and dynamic constraints at the hand–tool interface. Our framework (Fig. 2) addresses these challenges in three stages: (1) training an oracle policy in simulation with privileged observations and randomized force–torque perturbations, (2) distilling the oracle into a proprioceptive student policy for sim-to-real transfer, and (3) fine-tuning on hardware via a cross-attention tactile–force adaptation (CATFA) module trained with behavior cloning from real rollouts.

A. Oracle Policy Definition and Training

We define an oracle policy, π_{oracle} , with privileged observations to learn a base policy for manipulating in-hand articulated tools. The oracle policy is trained in simulation using PPO [55] with a curriculum of force–torque perturbations applied to the in-hand articulated tool, which gradually increases disturbance magnitude to emulate arbitrary gravity vectors and external tool contact dynamics to increase robustness, a method that is further discussed in Sec. III-A. At each timestep t , the oracle outputs absolute joint targets $u_t \leftarrow \pi_{oracle}(o_t)$ from privileged observations o_t . Ultimately, the privileged information will be removed through distillation for sim-to-real transfer, which is a more

efficient technique than directly learning a policy with only non-privileged information [56].

Initial State. The initial state of the articulated object is set using teleoperated demonstrations with a hand tracker (Manus gloves [57]) whenever the robotic hand fails to achieve a stable initial grasp, ensuring that rollouts consistently start from feasible hand–tool configurations despite variability in articulation poses.

Observations. The privileged observation at time t is

$$o_t = [q_t, \dot{q}_t, u_{t-1}, \theta_t^{art}, \dot{\theta}_t^{art}, x_t^{obj}, \dot{x}_t^{obj}, s_t, \tau_t^{raw}],$$

where $q_t \in \mathbb{R}^6$ and $\dot{q}_t \in \mathbb{R}^6$ denote the dexterous hand joint positions and velocities, considering only the active joint configuration (four finger joints, two thumb joints afforded by the Inspire Robotics hands used in this paper), $u_{t-1} \in \mathbb{R}^6$ is the previous target configuration, $x_t^{obj} \in \mathbb{R}^3$ and $\dot{x}_t^{obj} \in \mathbb{R}^3$ are the pose and velocity of the in-hand articulated object w.r.t. the robot base frame, $\tau_t^{raw} \in \mathbb{R}^6$ are the raw simulated joint force signals for all actuated DoFs, and $s_t \in \{0, 1\}^2$ is the binary one-hot articulation command specifying the target state of the tool (e.g., open or closed). Visual feedback is excluded, since these privileged states already provide full virtual object information sufficient for training without the added complexity of high-dimensional vision inputs [58].

Actions. At each step, the policy outputs absolute joint targets $u_t \in \mathbb{R}^6$ for the fingers of the hand. To improve stability and reduce vibrations in the hand, the executed command is smoothed with a light-handed exponential moving average:

$$\tilde{u}_t \leftarrow \alpha u_t + (1 - \alpha)u_{t-1}, \quad \alpha = 0.5. \quad (1)$$

Reward. The reward function is the sum of terms in Table I, balancing articulation progress with stability. The position r_t^{pos} and orientation r_t^{quat} terms minimize deviation from the initial pose. Task progress is promoted by the joint goal r_t^{goal} , which reduces error between θ_t^{art} and the commanded target $\theta_{s_t}^{target}$, and by the timer r_t^{timer} , which rewards maintaining the desired articulation state s_t . Incremental shaping r_t^{inc} provides staged bonuses as θ_t^{art} crosses thresholds in

Θ_{s_t} . Stability is enforced through the contact term r_t^{contact} , penalizing deviations between the actual number of finger links contacts n_t and the desired count n^* , and the slippage term r_t^{slip} , triggered when the object height h_t^{obj} falls below a threshold h_{min} . Finally, the action penalty r_t^{act} discourages large joint targets u_t .

Equation	Scale
$r_t^{\text{pos}} = -\ x_t^{\text{obj}} - x_0^{\text{obj}}\ _2^2$	500.0
$r_t^{\text{quat}} = -\ q_t^{\text{obj}} - q_0^{\text{obj}}\ _2^2$	5.0
$r_t^{\text{goal}} = - \theta_t^{\text{art}} - \theta_{s_t}^{\text{target}} $	10.0
$r_t^{\text{timer}} = \begin{cases} T_{t-1}^{\text{open}} + 1, & s_t = 1 \wedge \theta_t^{\text{art}} \geq \theta_{\text{open}}, \\ T_{t-1}^{\text{close}} + 1, & s_t = 0 \wedge \theta_t^{\text{art}} \leq \theta_{\text{close}}, \\ -1, & \text{otherwise} \end{cases}$	0.05
$r_t^{\text{inc}} = \sum_{\vartheta \in \Theta_{s_t}} w(\vartheta) \mathbf{1}\{\theta_t^{\text{art}} \text{ crosses } \vartheta\}$	1.0
$r_t^{\text{contact}} = n^* - n_t$	-0.1
$r_t^{\text{slip}} = \mathbf{1}\{h_t^{\text{obj}} < h_{\text{min}}\}$	-1.0
$r_t^{\text{act}} = -\ u_t\ _2^2$	-0.001

TABLE I: Reward function for the oracle policy.

Policy optimization with random walk perturbations.

To improve the robustness of the instrument grasp during articulation, external disturbances are simulated in a random walk process during training. At each step, external forces $F_t^{\text{ext}} \in \mathbb{R}^3$ and torques $\tau_t^{\text{ext}} \in \mathbb{R}^3$ applied to the hand and tool are updated as

$$\begin{aligned} F_t^{\text{ext}} &= \text{clip}(F_{t-1}^{\text{ext}} + \Delta F_t^{\text{ext}}, F_{\text{min}}, F_{\text{max}}), \\ \tau_t^{\text{ext}} &= \text{clip}(\tau_{t-1}^{\text{ext}} + \Delta \tau_t^{\text{ext}}, \tau_{\text{min}}, \tau_{\text{max}}), \end{aligned} \quad (2)$$

where ΔF_t^{ext} and $\Delta \tau_t^{\text{ext}}$ are sampled from uniform ranges and the values are clipped within specified bounds. A random walk is chosen in the force/torque space so that forces and torques can directionally accumulate over time and provide a wide coverage of potential disturbances. This enables covering forces and torques that emulate gravity, acceleration, and contact disturbances within a bounded domain. As shown in Fig. 3, policies trained with random-walk perturbations exhibit improved robustness under external disturbances, while the resulting joint configurations provide more stable securing of the articulated tool in both open and closed states.

B. Base Policy Distillation

Standard distillation methods like DAgger [59] are ineffective for articulated in-hand manipulation, as partially informed students π_{student} drop objects early and fail to explore; we instead distill from stable oracle rollouts π_{oracle} to obtain diverse training data. While visuotactile policies [54], [21] demonstrate promising performance in simulation, they exhibit a substantial sim-to-real gap due to occlusions and sensing discrepancies (see Sec. III-C (hardware sensing) for details). In contrast, proprioceptive feedback (q_t, s_t) is both stable in simulation and directly observable on hardware, making it the most reliable modality for transfer. To exploit this property, we first train an oracle policy π_{oracle} with full privileged state information in simulation, and then distill its actions into a student policy π_{student} that no longer relies on inaccessible states. The student is parameterized as a

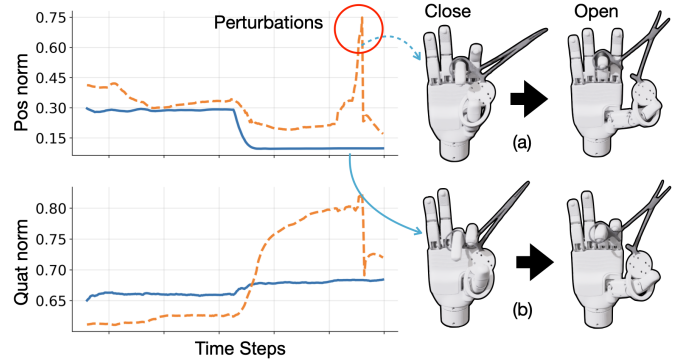


Fig. 3: Pose norm (top) and quaternion norm (bottom) of the articulated tool (surgical clamp). Blue: policy with perturbation optimization, which corresponds to (b); Orange: policy without random-walk perturbations, which corresponds to (a)

multilayer perceptron with hidden dimensions [256, 128, 64] and is defined as

$$\pi_{\text{student}}(\hat{u}_t | q_t, s_t) = \text{MLP}_{[256, 128, 64]}([q_t, s_t]) \quad (3)$$

where q_t denotes the reference geometry (joint configuration) and $s_t \in \{0, 1\}$ is the binary articulation command. We also retain the random-walk force–torque perturbations during training (Eq. 2), enabling the student to acquire robustness against gravity-induced and contact disturbances under quasi-static manipulation dynamics.

C. Online Adaptation via Cross-Attention Tactile Force Module (CATFA)

While the distilled base policy π_{student} provides a useful motion prior, it operates in an open-loop manner and cannot perceive or respond to real-time perturbations. This limitation is particularly problematic for articulated tools, where internal joint couplings and contact dynamics make in-hand rollout of tools more likely. Although domain randomization improves robustness in simulation, the absence of sensing prevents the policy from receiving real-time feedback on the object slip and corrective actions. To address this, we introduce a *Cross-Attention Tactile Force Adaptation (CATFA)* module that leverages real tactile and motor force inputs to learn the behavior of the base policy π_{student} while simultaneously acquiring a feedback mechanism for disturbance rejection.

Hardware Sensing. Each finger of the robot hand incorporates a series of resistive tactile skins that provide an array of quantized force readings $f_t^{\text{tact}} \in \mathbb{R}^{36 \times 44}$ to process the finger pads. These pads were found to be highly unreliable in consistent sensing, and we found that adding a foam-plate-pad layer (Fig. 4) that redistributes local contact loads across neighboring taxels to increase the sensitivity and repeatability of measuring contact. We additionally measure joint forces $\tau_t^{\text{motor}} \in \mathbb{R}^6$ from motor current sensing, where extension is governed by passive spring return and flexion by the geared actuators. In simulation, the oracle policy π_{oracle} relies on raw actuator estimates τ_t^{raw} , which differ from hardware signals τ_t^{motor} due to transmission effects (gear ratio, friction, backlash, compliance, and sensor gains).

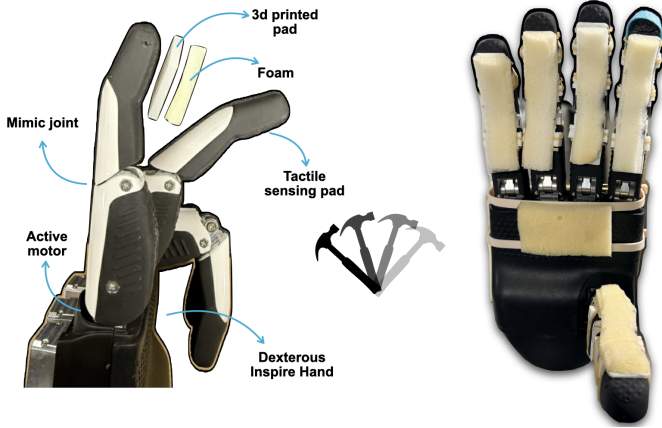


Fig. 4: Inspire hand with augmented tactile structure: a 3D-printed pad and foam layer enhance sensitivity, with motor and mimic joints shown. Motor torques τ_t^{motor} are computed only from the active joints.

Because reproducing these dynamics would require detailed system identification and calibration, we avoid simulating τ_t^{motor} and instead incorporate the real tactile readings f_t^{tact} and motor-derived forces τ_t^{motor} directly into the adaptation module (CATFA).

Model Architecture. CATFA augments the frozen base policy π_{student} with a sensor-driven refinement network. At each timestep t , the base policy π_{student} produces an internal intent embedding $z_t \in \mathbb{R}^{64}$ from its final MLP layer. In parallel, the tactile array $f_t^{\text{tact}} \in \mathbb{R}^{36 \times 44}$ is processed by a convolutional encoder to yield a compact feature vector $\phi_t^{\text{tact}} \in \mathbb{R}^{64}$. In contrast, motor force readings $\tau_t^{\text{motor}} \in \mathbb{R}^6$ are mapped through a two-layer MLP to produce $\phi_t^{\text{force}} \in \mathbb{R}^{64}$. These sensor encodings are concatenated into $F_t = [\phi_t^{\text{tact}}, \phi_t^{\text{force}}] \in \mathbb{R}^{2 \times 64}$. A multi-head cross-attention module (MHA, with 8 heads and embed dimension 64) fuses intent and sensor signals by querying with z_t against F_t , where z_t is the key input representing the learned proprioception embeddings from the original student policy and F_t are the key and value inputs providing the feedback mechanism necessary to reach the state from the sensor data.

$$\tilde{z}_t = \text{MHA}(z_t, F_t, F_t) \in \mathbb{R}^{64} \quad (4)$$

The attended embedding \tilde{z}_t conditions a lightweight adaptor network (two-layer MLP) that outputs the final joint targets $\hat{u}_t \in \mathbb{R}^4$. This adaptor is trained via behavior cloning on successful real-world rollouts, enabling online refinement of the sim-to-real base policy π_{student} under articulated, contact-rich dynamics.

Training Adaptation. We fine-tune the system by executing the sim-to-real base policy π_{student} on the physical robot under random disturbances and collecting fewer than 50 successful rollouts, where success or failure is annotated via human feedback. Each rollout spans a horizon of 2000 time steps and contains multiple open/close phases, with the articulation command s_t switching after random intervals (e.g., from $t = 50$ to $t = 250$ and beyond). This procedure exposes the policy to diverse articulation states and transitions, improving robustness to state changes. CATFA is

Policy	Articulated Tool	Succ (%)	TipErr (O)	TipErr (C)
<i>Simulation (Oracle)</i>				
	Surgical clamp	100	57.26 ± 0.63	0.008 ± 0.001
	Tong	100	51.55 ± 2.93	17.23 ± 1.45
	Plier	100	17.45 ± 1.20	13.34 ± 2.10
	Laparoscopic tool	100	99.31 ± 2.2494	67.62 ± 1.58
	Stapler	100	22.88 ± 1.44	0.000 ± 0.000
<i>Sim-to-Real (Student)</i>				
	Surgical clamp	20	25.8 ± 16.3	30.4 ± 21.8
	Tong	100	64.23 ± 0.97	29.17 ± 1.26
	Plier	30	7.73 ± 5.87	3.68 ± 0.21
	Laparoscopic tool	100	109.31 ± 1.75	76.98 ± 1.52
	Stapler	100	5.32 ± 0.40	1.03 ± 0.87
<i>Proprioception BC</i>				
	Surgical clamp	90	44.6 ± 0.66	0.0 ± 0.0
	Tong	100	51.55 ± 0.87	32.64 ± 1.7
	Plier	70	9.81 ± 0.30	9.06 ± 0.36
	Laparoscopic tool	100	107.39 ± 1.48	75.07 ± 2.06
	Stapler	100	5.08 ± 0.48	0.6 ± 0.5
<i>CATFA (Ours)</i>				
	Surgical clamp	100	54.5 ± 0.8	0.0 ± 0.0
	Tong	100	51.23 ± 0.36	28.31 ± 0.91
	Plier	100	11.28 ± 0.76	3.12 ± 0.16
	Laparoscopic tool	100	109.31 ± 1.75	78.37 ± 1.72
	Stapler	100	5.32 ± 0.17	0.09 ± 0.01

TABLE II: Quantitative evaluation on articulated tools. Metrics: **Succ** — **TipErr(O)** — **TipErr(C)**. TipErr(O) is the tool-tip distance error in the open state (mm), where larger values indicate better opening, and TipErr(C) is the error in the closed state (mm), where lower values indicate better closure. Due to differences in object scale, these measurements may be more consistent in simulation than in the real world. Only the oracle policy is evaluated in simulation; all other policies are executed on the real robot.

trained via behavior cloning on a small human-labeled successful real-world rollouts. Formally, given demonstrations $\mathcal{D} = \{(q_t, s_t, u_t)\}$, with oracle actions u_t , the student policy π_{student} minimizes

$$\mathcal{L}_{\text{BC}} = \mathbb{E}_{(q_t, s_t, u_t) \sim \mathcal{D}} [\|u_t - \pi_{\text{student}}(q_t, s_t)\|_2^2] \quad (5)$$

enabling efficient sim-to-real adaptation under contact-rich dynamics. While the base policy π_{student} remains frozen, allowing CATFA to inherit the motion prior and acquire a real-time feedback mechanism.

IV. EXPERIMENTS

A. Articulated tools set

We evaluate our approach on five articulated tools, each modeled with a single revolute joint and instantiated in both simulation and the real world (Fig. 5). To improve robustness under sim-to-real transfer, we randomize object mass, surface friction, and material properties in simulation. Although the simulated joints capture the intended kinematics, they do not fully replicate real-world mechanics, creating a domain gap. To address scale differences, we attach simple mechanical fixtures so the objects fit the dexterous hand, which is about 1.4 times larger than an average human hand. This setup provides a controlled yet challenging benchmark for articulated in-hand manipulation.

B. Hardware Setup

We use the Inspire Hand, a dexterous robotic hand with 6 active DoFs (one per finger, two for thumb) and 6 mimic joints that follow the motion of the other joints. Joint targets

Policy	Clamp		Plier		Laparoscopic tool	
	Open	Close	Open	Close	Open	Close
Proprioception BC	0.083 ± 0.02	0.033 ± 0.017	0.047 ± 0.019	0.061 ± 0.021	0.242 ± 0.096	0.029 ± 0.067
Sim-to-Real (Student)	0.056 ± 0.04	0.083 ± 0.038	0.045 ± 0.018	0.043 ± 0.018	0.139 ± 0.135	0.076 ± 0.044
CATFA (Ours)	0.044 ± 0.021	0.029 ± 0.015	0.15 ± 0.035	0.04 ± 0.015	0.159 ± 0.083	0.033 ± 0.038

TABLE III: Perturbation analysis across three articulated tools in open and closed states. Each cell reports the **Mean Deviation** (position in meters). Metrics are computed from pose and quaternion norms while the Franka executes a pre-defined random trajectory with injected external perturbations.

Values are mean ± std over runs (lower is better).



Fig. 5: Articulated tools used in experiments: real-world examples (top) and simulated counterparts (bottom). The axis denotes the articulation rotation axis. These tools span a wide range of articulation types and gripping strategies, capturing diverse kinematic structures and manipulation provisions.

are commanded at 30 Hz and tracked by a low-level PD controller at 120 Hz. Tactile sensing runs at 75 Hz using a resistive array of 36×44 taxels, with additional force measurements available at all active joints. The hand is covered with a nitrile glove to improve textural consistency. The initial grasp configurations for tool manipulation are collected using Manus MetaGloves Pro [57], as described in Sec. III-A. The tactile sensing augmentation is detailed in Sec. III-C and Fig. 4.

C. Simulation

We use the IsaacLab [60] simulator to train our policy. Each environment contains the robot hand with articulated tools spawned with an initial state. The simulation runs at 120 Hz with a control decimation factor of 3, resulting in an effective control frequency of 40 Hz. Each episode lasts for 2000 simulation steps (approximately 50 s) and terminates if the object leaves the workspace due to a collision, if the object falls from the hand, or if the maximum episode length is reached. To approximate contact dynamics, we apply convex decomposition for more complex geometries and use convex hulls for simpler objects. For parallelization, 8192 environments were run headless on a single Nvidia RTX 4090. Depending on the object collision geometry, a

single articulated tool takes around 4-12 hours of training.

D. Ablation Study

We perform two sets of ablation studies to evaluate the contribution of tactile and force feedback. In the first study, we compare (i) the sim-to-real base policy π_{student} , (ii) the CATFA-augmented policy, and (iii) a behavior-cloned policy using only proprioceptive inputs (no tactile or force signals). Performance is measured on approximately 10 real-world rollouts per object by recording the articulation joint angle after each open/close phase and averaging across trials. Success is defined as maintaining the commanded open or closed state (angle above or below a threshold) throughout the episode. In the second study, we attach the dexterous hand to a Franka arm and execute predefined trajectories with randomized accelerations to emulate motion-planning-induced perturbations. We evaluate the same three policies by tracking the tool pose with ArUco markers and measuring the error between the tool pose and the desired end-effector pose. This setting quantifies robustness under dynamic perturbations during in-hand manipulation.

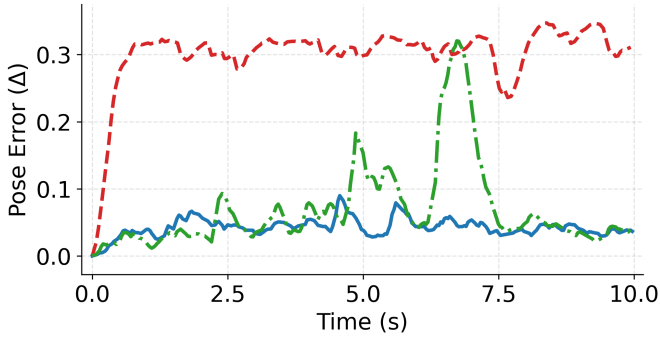
V. RESULTS

An overview of our pipeline is shown in Fig. 2. Our experiments evaluate the effectiveness of the proposed CATFA module for sim-to-real adaptation compared against proprioception-based behavior cloning baselines.

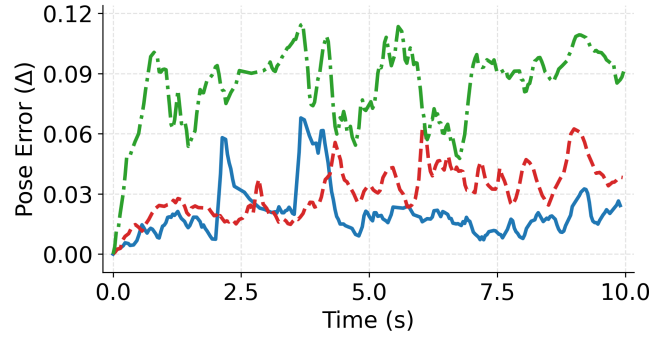
Baselines. We compare against two baselines: (1) a behavior cloning (BC) policy trained without tactile and force inputs for adaptation, using only proprioception; and (2) the distilled sim-to-real base policy π_{student} directly deployed on hardware, with limited fine-tuning to partially reduce the sim-to-real gap.

Real-world evaluation. We test policies on five articulated tools shown in Fig. 5. Quantitative evaluation is conducted on five in-domain objects, while qualitative demonstrations are shown on additional tools with variations in weight, scale, and geometry to assess generalization, which is shown on our website. For all tasks, success is defined based on maintaining articulation angle thresholds across multiple open–close cycles within an episode, and it is shown in Table II. CATFA consistently outperforms both baselines in maintaining stable articulation under perturbations.

Robustness to perturbations. To evaluate robustness, we execute a pre-defined random manipulation trajectory on the Franka hand–tool setup, incorporating random accelerations and external perturbations. As reported in Table III, pose error is measured by jointly considering position and



(a) Closed trajectory comparison



(b) Open trajectory comparison

Fig. 6: Trajectory metric comparison (translation + quaternion error, EMA with $\alpha = 0.25$). (a) Closed-state trajectories. (b) Open-state trajectories. Solid Blue: CATFA (ours) with smoother, lower deviations; dashed orange: Proprioceptive BC over Sim-to-Real; dotted-dashed green: Sim-to-Real Policy.

quaternion deviations, since these are inherently coupled. Furthermore, Fig. 6b shows that the CATFA policy produces smoother trajectories with significantly lower deviation than baselines in both open and closed states. **Simulation validation.** In simulation, we further compare policies trained with and without random walk perturbations (Eq. 2). Policies trained with perturbations exhibit improved stability under external disturbances, confirming that perturbation-augmented training contributes to robustness that transfers to hardware.

VI. DISCUSSION & CONCLUSION

Our research demonstrates a robust framework for learning in-hand tool articulation, yielding several key insights. We established that structured initialization is crucial for aligning grasps with tool joints and that simulation is vital for discovering complex, contact-rich manipulation skills. Our findings also reveal that while visuotactile policies face a significant sim-to-real transfer gap, policies based on proprioception provide a reliable bridge for transferring skills from simulation to hardware. These proprioceptive policies, refined with just a few real-world tactile and motor torque rollouts, achieve robust generalization.

These findings present a powerful paradigm for developing robotic manipulation skills that can serve as foundational ‘skill primitives’ for large-scale models. A high-level planner, such as a large language model, could command these policies to execute precise, low-level tasks. Furthermore, the modular nature of our cross-attention adaptor offers inherent extensibility for adding new sensory modalities. This architecture provides a clear pathway for integrating novel sensors in the future to handle even more complex tasks by simply training new, specialized adaptors.

Limitations The current policy is restricted to binary articulation commands $s_t \in \{0, 1\}$, limiting applicability to tools with more complex or continuous joints. Hardware fine-tuning remains sensitive to motor torque scaling and control frequency mismatches between simulation and the geared, spring-assisted hand. Moreover, the simulator does not capture motor-spring coupling during extension, constraining sim-to-real fidelity.

REFERENCES

- [1] S. Atar, X. Liang, C. Joyce, F. Richter, W. Ricardo, C. Goldberg, P. Suresh, and M. Yip, “Humanoids in hospitals: A technical study of humanoid robot surrogates for dexterous medical interventions,” 2025.
- [2] H. Qi, B. Yi, M. Lambeta, Y. Ma, R. Calandra, and J. Malik, “From simple to complex skills: The case of in-hand object reorientation,” 2025.
- [3] J. Wang, Y. Yuan, H. Che, H. Qi, Y. Ma, J. Malik, and X. Wang, “Lessons from learning to spin ‘pens’,” 2024.
- [4] W. Hu, B. Huang, W. W. Lee, S. Yang, Y. Zheng, and Z. Li, “Dexterous in-hand manipulation of slender cylindrical objects through deep reinforcement learning with tactile sensing,” *Robotics and Autonomous Systems*, vol. 186, p. 104904, 2025.
- [5] M. Yu, Y. Jiang, C. Chen, Y. Jia, and X. Li, “Robotic in-hand manipulation for large-range precise object movement: The rgmc champion solution,” 2025.
- [6] F. Burget, A. Hornung, and M. Bennewitz, “Whole-body motion planning for manipulation of articulated objects,” in *2013 IEEE International Conference on Robotics and Automation*, pp. 1656–1662, 2013.
- [7] Y. Liu, Y. Yang, Y. Wang, X. Wu, J. Wang, Y. Yao, S. Schwertfeger, S. Yang, W. Wang, J. Yu, X. He, and Y. Ma, “Realdex: Towards human-like grasping for robotic dexterous hand,” in *Proceedings of the Thirty-Third International Joint Conference on Artificial Intelligence, IJCAI-2024*, p. 6859–6867, International Joint Conferences on Artificial Intelligence Organization, Aug. 2024.
- [8] Z. Luo, J. Cao, S. Christen, A. Winkler, K. Kitani, and W. Xu, “Omnigrasp: Grasping diverse objects with simulated humanoids,” 2025.
- [9] A. Werby, M. Büchner, A. Röfer, C. Huang, W. Burgard, and A. Valada, “Articulated object estimation in the wild,” 2025.
- [10] R. Chu, Z. Liu, X. Ye, X. Tan, X. Qi, C.-W. Fu, and J. Jia, “Command-driven articulated object understanding and manipulation,” in *2023 IEEE/CVF Conference on Computer Vision and Pattern Recognition (CVPR)*, pp. 8813–8823, 2023.
- [11] T. Asfour, P. Azad, N. Vahrenkamp, K. Regenstein, A. Bierbaum, K. Welke, J. Schröder, and R. Dillmann, “Toward humanoid manipulation in human-centred environments,” *Robotics and Autonomous Systems*, vol. 56, no. 1, pp. 54–65, 2008. Human Technologies: “Know-how”.
- [12] T. Chen, M. Tippur, S. Wu, V. Kumar, E. Adelson, and P. Agrawal, “Visual dexterity: In-hand reorientation of novel and complex object shapes,” *Science Robotics*, vol. 8, Nov. 2023.
- [13] H. Qi, A. Kumar, R. Calandra, Y. Ma, and J. Malik, “In-hand object rotation via rapid motor adaptation,” 2022.
- [14] H. Choi, C. Crump, C. Duriez, A. Elmquist, G. Hager, D. Han, F. Hearl, J. Hodgins, A. Jain, F. Leve, et al., “On the use of simulation in robotics: Opportunities, challenges, and suggestions for moving forward,” *Proceedings of the National Academy of Sciences*, vol. 118, no. 1, p. e1907856118, 2021.
- [15] S. Atar, Y. Li, M. Grotz, M. Wolf, D. Fox, and J. Smith, “Optigrasp: Optimized grasp pose detection using rgb images for warehouse picking robots,” 2024.

- [16] B. Yang, S. Atar, M. Grotz, B. Boots, and J. Smith, "DYNAMO-GRASP: DYNAMics-aware optimization for GRASP point detection in suction grippers," in *7th Annual Conference on Robot Learning*, 2023.
- [17] N. Jawale, B. Boots, B. Sundaralingam, and M. Bhardwaj, *Dynamic Non-Prehensile Object Transport via Model-Predictive Reinforcement Learning*. 2025 IEEE International Conference on Robotics and Automation (ICRA), IEEE, 2025-5-19.
- [18] S. Wang, M. Lambeta, P.-W. Chou, and R. Calandra, "Tacto: A fast, flexible, and open-source simulator for high-resolution vision-based tactile sensors," *IEEE Robotics and Automation Letters*, vol. 7, p. 3930–3937, Apr. 2022.
- [19] Z.-H. Yin, B. Huang, Y. Qin, Q. Chen, and X. Wang, "Rotating without seeing: Towards in-hand dexterity through touch," 2023.
- [20] J. Yin, H. Qi, J. Malik, J. Pikul, M. Yim, and T. Hellebrekers, "Learning in-hand translation using tactile skin with shear and normal force sensing," 2025.
- [21] H. Qi, B. Yi, S. Suresh, M. Lambeta, Y. Ma, R. Calandra, and J. Malik, "General in-hand object rotation with vision and touch," 2023.
- [22] Q. L. Lidec, W. Jallet, L. Montaut, I. Laptev, C. Schmid, and J. Carpentier, "Contact models in robotics: a comparative analysis," 2024.
- [23] B. Acosta, W. Yang, and M. Posa, "Validating robotics simulators on real-world impacts," 2022.
- [24] T. Lin, Y. Zhang, Q. Li, H. Qi, B. Yi, S. Levine, and J. Malik, "Learning visuotactile skills with two multifingered hands," 2024.
- [25] J. Li, Y. Zhu, Y. Xie, Z. Jiang, M. Seo, G. Pavlakos, and Y. Zhu, "Okami: Teaching humanoid robots manipulation skills through single video imitation," 2024.
- [26] X. Zhang, Y. Wang, R. Wu, K. Xu, Y. Li, L. Xiang, H. Dong, and Z. He, "Adaptive articulated object manipulation on the fly with foundation model reasoning and part grounding," 2025.
- [27] Y. Lin, Y.-L. Wei, H. Liao, M. Lin, C. Xing, H. Li, D. Zhang, M. Cutkosky, and W.-S. Zheng, "Typetele: Releasing dexterity in teleoperation by dexterous manipulation types," 2025.
- [28] M. Xu, H. Zhang, Y. Hou, Z. Xu, L. Fan, M. Veloso, and S. Song, "Dexumi: Using human hand as the universal manipulation interface for dexterous manipulation," 2025.
- [29] G. Li, R. Wang, P. Xu, Q. Ye, and J. Chen, "The developments and challenges towards dexterous and embodied robotic manipulation: A survey," 2025.
- [30] L. P. Kaelbling and T. Lozano-Pérez, "Hierarchical task and motion planning in the now," in *2011 IEEE International Conference on Robotics and Automation*, pp. 1470–1477, 2011.
- [31] A. G. Barto and S. Mahadevan, "Recent advances in hierarchical reinforcement learning," *Discrete Event Dynamic Systems*, vol. 13, pp. 41–77, 2003.
- [32] G. Seneviratne, K. Weerakoon, M. Elnoor, V. Rajgopal, H. Varatharajan, M. K. M. Jaffar, J. Pusey, and D. Manocha, "Cross-gait: Cross-attention-based multimodal representation fusion for parametric gait adaptation in complex terrains," 2025.
- [33] J.-P. Saut, A. Sahbani, S. El-Khoury, and V. Perdereau, "Dexterous manipulation planning using probabilistic roadmaps in continuous grasp subspaces," pp. 2907 – 2912, 10 2007.
- [34] L. Han, Y. Guan, Z. Li, Q. Shi, and J. J. Trinkle, "Dextrous manipulation with rolling contacts," pp. 992 – 997 vol.2, 05 1997.
- [35] O. M. Andrychowicz, B. Baker, M. Chociej, R. Józefowicz, B. McGrew, J. Pachocki, A. Petron, M. Plappert, G. Powell, A. Ray, J. Schneider, S. Sidor, J. Tobin, P. Welinder, L. Weng, and W. Zaremba, "Learning dexterous in-hand manipulation," *The International Journal of Robotics Research*, vol. 39, no. 1, pp. 3–20, 2020.
- [36] Y. Bai, W. Yu, and C. K. Liu, "Dexterous manipulation of cloth," in *Proceedings of the 37th Annual Conference of the European Association for Computer Graphics*, EG '16, (Goslar, DEU), p. 523–532, Eurographics Association, 2016.
- [37] I. Mordatch, Z. Popović, and E. Todorov, "Contact-invariant optimization for hand manipulation," in *Proceedings of the ACM SIGGRAPH/Eurographics Symposium on Computer Animation*, SCA '12, (Goslar, DEU), p. 137–144, Eurographics Association, 2012.
- [38] *Proceedings of the 1986 IEEE International Conference on Robotics and Automation, San Francisco, California, USA, April 7-10, 1986*, IEEE, 1986.
- [39] F. Zhao, B. Huang, M. Li, M. Li, Z. Fu, Z. Lei, and M. Li, "A novel tactile palm for robotic object manipulation," in *Intelligent Robotics and Applications: 16th International Conference, ICIRA 2023, Hangzhou, China, July 5–7, 2023, Proceedings, Part V*, (Berlin, Heidelberg), p. 81–92, Springer-Verlag, 2023.
- [40] S. Patidar, A. Sieler, and O. Brock, "In-hand cube reconfiguration: Simplified," pp. 8751–8756, 10 2023.
- [41] OpenAI, I. Akkaya, M. Andrychowicz, M. Chociej, M. Litwin, B. McGrew, A. Petron, A. Paino, M. Plappert, G. Powell, R. Ribas, J. Schneider, N. Tezak, J. Tworek, P. Welinder, L. Weng, Q. Yuan, W. Zaremba, and L. Zhang, "Solving rubik's cube with a robot hand," 2019.
- [42] A. Bhatt*, A. Sieler*, S. Puhlmann, and O. Brock, "Surprisingly robust in-hand manipulation: An empirical study," in *Robotics: Science and Systems XVII*, RSS2021, Robotics: Science and Systems Foundation, July 2021.
- [43] S. Patidar, A. Sieler, and O. Brock, "In-hand cube reconfiguration: Simplified," 2023.
- [44] Y. Qin, B. Huang, Z.-H. Yin, H. Su, and X. Wang, "Dexpoint: Generalizable point cloud reinforcement learning for sim-to-real dexterous manipulation," 2022.
- [45] A. Handa, A. Allshire, V. Makoviychuk, A. Petrenko, R. Singh, J. Liu, D. Makoviichuk, K. V. Wyk, A. Zhurkevich, B. Sundaralingam, Y. Narang, J.-F. Lafleche, D. Fox, and G. State, "Dextreme: Transfer of agile in-hand manipulation from simulation to reality," 2024.
- [46] M. Yang, C. Lu, A. Church, Y. Lin, C. Ford, H. Li, E. Psomopoulou, D. A. W. Barton, and N. F. Lepora, "Anyrotate: Gravity-invariant in-hand object rotation with sim-to-real touch," 2024.
- [47] Y. Wang, Z. Wang, M. Nakura, P. Bhowal, C.-L. Kuo, Y.-T. Chen, Z. Erickson, and D. Held, "Articubot: Learning universal articulated object manipulation policy via large scale simulation," 2025.
- [48] Z. Xu, Z. He, and S. Song, "Universal manipulation policy network for articulated objects," *IEEE Robotics and Automation Letters*, vol. 7, p. 2447–2454, Apr. 2022.
- [49] X. Wang, T. Chen, Q. Yu, T. Xu, Z. Chen, Y. Fu, Z. He, C. Lu, Y. Mu, and P. Luo, "Articulated object manipulation using online axis estimation with sam2-based tracking," 2025.
- [50] W. Xu, Y. Zhao, W. Guo, and X. Sheng, "Hierarchical reinforcement learning for articulated tool manipulation with multifingered hand," 2025.
- [51] N. Jawale, N. Kaur, A. Santoso, X. Hu, and X. Chen, *Learned Slip-Detection-Severity Framework using Tactile Deformation Field Feedback for Robotic Manipulation*. 2024 IEEE/RSJ International Conference on Intelligent Robots and Systems (IROS), IEEE, 2024-10-14.
- [52] S. Cremer, M. N. Saadatzi, I. B. Wijayasinghe, S. K. Das, M. H. Saadatzi, and D. O. Popa, "Skinsim: A design and simulation tool for robot skin with closed-loop phri controllers," *IEEE Transactions on Automation Science and Engineering*, vol. 18, no. 3, pp. 1302–1314, 2021.
- [53] Z. Kappassov, J.-A. Corrales-Ramon, and V. Perdereau, "Simulation of tactile sensing arrays for physical interaction tasks," in *2020 IEEE/ASME International Conference on Advanced Intelligent Mechatronics (AIM)*, pp. 196–201, 2020.
- [54] Y. Yuan, H. Che, Y. Qin, B. Huang, Z.-H. Yin, K.-W. Lee, Y. Wu, S.-C. Lim, and X. Wang, "Robot synesthesia: In-hand manipulation with visuotactile sensing," 2024.
- [55] J. Schulman, F. Wolski, P. Dhariwal, A. Radford, and O. Klimov, "Proximal policy optimization algorithms," 2017.
- [56] A. Kumar, Z. Fu, D. Pathak, and J. Malik, "Rma: Rapid motor adaptation for legged robots," 2021.
- [57] MANUS Technology Group, "High-precision hand tracking & mocap gloves — manus." <https://www.manus-meta.com/>, 2025. Accessed: 2025-09-13.
- [58] T. Mu, Z. Li, S. W. Strzelecki, X. Yuan, Y. Yao, L. Liang, and H. Su, "When should we prefer state-to-visual dagger over visual reinforcement learning?," in *Proceedings of the Thirty-Ninth AAAI Conference on Artificial Intelligence and Thirty-Seventh Conference on Innovative Applications of Artificial Intelligence and Fifteenth Symposium on Educational Advances in Artificial Intelligence*, AAAI'25/IAAI'25/EAAI'25, AAAI Press, 2025.
- [59] S. Ross, G. J. Gordon, and J. A. Bagnell, "A reduction of imitation learning and structured prediction to no-regret online learning," 2011.
- [60] M. Mittal, C. Yu, Q. Yu, J. Liu, N. Rudin, D. Hoeller, J. L. Yuan, R. Singh, Y. Guo, H. Mazhar, A. Mandlekar, B. Babich, G. State, M. Hutter, and A. Garg, "Orbit: A unified simulation framework for interactive robot learning environments," *IEEE Robotics and Automation Letters*, vol. 8, no. 6, pp. 3740–3747, 2023.